Journal of Cellular Biochemistry 67:409–421 (1997)

Inhibition of Cytoskeletal Reorganization Stimulates Actin and Tubulin Syntheses During Injury-Induced Cell Migration in the Corneal Endothelium

Sheldon R. Gordon* and Renee M. Buxar

Department of Biological Sciences, Oakland University, Rochester, Michigan 48309

Abstract A single layer of squamous epithelial cells termed the "endothelium" resides upon its natural basement membrane (Descemet's membrane) along the posterior surface of the vertebrate cornea. A well-defined circular freeze injury to the center of the tissue exposes the underlying basement membrane and results in the directed migration of surrounding cells into the wound center. This cellular translocation is characterized by the reorganization of the actin and tubulin cytoskeletons. During migration, circumferential microfilament bundles are replaced by prominent stress fibers while microtubules, observed as delicate lattices in non-injured cells, become organized into distinct web-like patterns. To determine whether this cytoskeletal reorganization requires actin or tubulin synthesis, injured rabbit endothelia were organ cultured for various times and metabolically labeled with ^{35}S-methionine/cystine (250 µCi/ml) for the final 6 h of each experiment. Analysis of actin and tubulin immunoprecipitates indicated no significant increases in ^{35}S incorporation occurred during the course of wound repair when compared to isotope incorporation in noninjured tissues. However, when cytoskeletal reorganization was hampered, either by pre-treating tissues with 7 µM phalloidin to stabilize their circumferential microfilament bundles, or culturing in the presence of 10^{-8}M colchicine to dissociate microtubules, ^{35}S incorporation increased significantly into both actin and tubulin immunoprecipitates at 48 h post-injury. Furthermore, in both cases, exposure to actinomycin D substantially suppressed isotope incorporation. These results indicate that cytoskeletal rearrangement of microfilaments and microtubules during wound repair, in corneal endothelial cells migrating along their natural basement membrane, utilizes existing actin and tubulin subunits for filament reorganization. Disrupting this disassembly/reassembly process prevents cytoskeletal restructuring and leads to the subsequent initiation of actin and tubulin syntheses, as a result of increased transcriptional activity. J. Cell. Biochem. 67:409–421, 1997.

Key words: corneal endothelium; actin; tubulin; upregulation; autoregulation; migration; wound repair

The posterior surface of the vertebrate cornea is lined by a single layer of very squamous epithelial cells that are termed the corneal "endothelium." They reside on their natural basement membrane, termed Descemet's membrane. These cells serve as a transport epithelia whose function is to maintain corneal deturgescence and hence transparency.

Cells of the adult corneal endothelium are mitotically inactive, and the entire cell population resides in the G_o phase of the cell cycle [Gordon and Rothstein, 1978]. Trauma to the tissue, such as a circular freeze injury, provides the stimulus for cells around the wound region to initiate macromolecular synthesis, traverse the cell cycle, divide, and migrate into the wound, along Descemet's membrane [Gordon, 1994]. Previous studies have shown that cell migration is the major mechanism involved in corneal endothelial wound repair [Doughman et al., 1976; Gordon and Rothstein, 1982]. However, the underlying mechanisms governing cell movement along natural basement membranes are less well characterized. For example, rat corneal endothelial cells synthesize and secrete extracellular matrix proteins during wound repair [Gordon, 1988; Munjal et al., 1990] despite residing on and moving along Descemet's membrane after an injury.

The initiation of endothelial migration is also accompanied by cytoskeletal alterations. The actin cytoskeleton of these cells is characterized by the presence of a distinct circumferen-

Contract grant sponsor: Oakland University Research Excellence Program in Biochemistry and Biotechnology.

*Correspondence to: Sheldon R. Gordon, Ph.D., Department of Biological Sciences, Oakland University, Rochester, MI 48309-4476. E-mail: srgordon@oakland.edu

Received 23 July 1997; Accepted 13 August 1997

tial microfilament bundle (CMB) [Gordon et al., 1982; Gordon, 1990; Gordon and Staley, 1990] that is associated with apical junctional complexes [Barry et al., 1995]. Injury to the tissue results in the reorganization of CMBs as cells initiate movement into the wound region to reestablish the monolayer [Gordon and Staley, 1990; Petroll et al., 1995; 1997]. The extent of actin reorganization and migration in this system correlates with the size of the wound [Ichijima et al., 1993]. In small endothelial injuries, cells maintain contact with adjacent neighbors during the repair process and those bordering the wound edge display decreased F-actin while retaining their CMBs [Petroll et al., 1995], reminiscent to that reported for small wounds in cultured vascular endothelium [Wong and Gotlieb, 1988]. In some regions along the wound edge, microfilament arcs around the injury have also been reported [Petroll et al., 1995], suggestive of "purse string" wound closure [Martin and Lewis, 1992; Bement et al., 1993]. In contrast, larger transcorneal freeze injuries result in the loss of cell-to-cell contacts [Munjal et al., 1990], that are associated with a dynamic reorganization of the actin cytoskeleton to form stress fibers in migrating cells [Gordon et al., 1982; Gordon and Staley, 1990; Ichijima et al., 1993]. Similar microfilament changes have been confirmed in vascular endothelium [Gabbiani et al., 1983; Gotlieb et al., 1984; Rogers et al., 1989; Ettenson and Gotlieb, 1993b], intestinal and respiratory epithelium [Zahm et al., 1991; Nusrat et al., 1992], and in the organ cultured retinal pigment epithelium [Hergot et al., 1989]. Recently, Lee et al. [1996] described three sequential stages of microfilament reorganization in response to the wounding of vascular endothelial monolayer cultures. Initially, actin was arranged as CMBs, but following an injury these disappear and central microfilaments appear that parallel the wound. This stage is transient and soon microfilaments assume a perpendicular orientation to the wound as movement is initiated. Collectively, these data indicate that in many systems, the cellular response to wounding is accompanied by a distinctive rearrangement of the actin cytoskeleton into stress fibers that are associated with cell migration.

Alterations in the microtubule pattern of corneal endothelial cells during the transition from a resting to a migratory state are not as dramatic as microfilament changes. Initially, microtubules appear in a delicate filamentous lattice that, following injury, forms a web-like pattern [Gordon and Staley, 1990]. Accompanying this change is a translocation of the microtubule organizinging center (MTOC) to the anterior portion of the cell [Gordon, 1994]. Similar results are observed in vascular endothelium, both in vitro [Gotlieb et al., 1984] and in the organ cultured system [Rogers et al., 1989]. Mechanisms underlying MTOC translocation are not fully understood, although it has been shown to depend on transcriptional activity occurring shortly after wounding [Ettenson and Gotlieb, 1993a]. The relocation of the MTOC appears to correlate with directed cell migration and interfering with this process retards wound repair [Ettenson and Gotlieb, 1993a]. Similarly, in the corneal endothelium, MTOC translocation may be coupled not only with directed migration but also to the polarized secretion of extracellular matrix protein. Disrupting microtubule integrity with colchicine prevents not only the deposition of fibronectin, but results in the restriction of cell movement [Sabet and Gordon, 1989; Gordon and Staley, 1990]. In this present study, we have investigated cytoskeletal changes in the organ cultured corneal endothelium during wound repair. Specifically, we examined whether microfilament and microtubule alterations during cell migration resulted from the reorganization of the pre-existing filaments or the synthesis of new actin and tubulin.

MATERIALS AND METHODS

Injury and Organ Culture

Eyes were isolated from New Zealand white rabbits (2.2 kg) and corneas given a circular transcorneal freeze injury (approximately 5 mm diameter) using a tapered hollow brass cone containing an ethanol/dry ice mixture (−70°C). Corneas were carefully dissected away from the globe, maintaining a 1-mm wide scleral rim to facilitate handling. In phalloidin pre-treatment experiments, endothelia were given a direct freeze injury using a stainless steel circular probe pre-cooled to −70°C in ethanol and dry ice. Corneas were cultured endothelial side up in basal medium Eagle (BME) (Sigma Cemical Co., St. Louis, MO) supplemented with 10% rabbit serum (Sigma) and 40 μg/ml gentamicin (Sigma) and incubated at 37°C in a humidified atmosphere of 5% CO_2 and 95% air. For some experiments involving tubulin cytoskeletal reorganization, the medium was also supplemented with 10^{-8}M colchicine (Sigma). For other experi-

ments, tissues were incubated in medium supplemented with 0.05 µg/ml actinomycin D (Sigma) from 18–48 h post-injury. For metabolic labeling, tissues were transferred into minimal essential medium Eagle without cystine or methionine (ICN Pharmaceuticals, Costa Mesa, CA) containing 250 µCi/ml ^{35}S Trans® (ICN) for the final 6 h of incubation.

Phalloidin Pre-Treatment

In some experiments, endothelial microfilaments were exposed to phallotoxins prior to wounding. For this, corneal endothelia were organ cultured in BME containing 7.5 µM phalloidin, either non-labeled or labeled with rhodamine (TRITC) for 20 h prior to receiving an injury. At the conclusion of the experiments, tissues exposed to non-labeled phalloidin were fixed and stained with TRITC-phalloidin. In other cases, tissues pre-treated with labeled phalloidin were fixed and processed for observation by fluorescence microscopy.

Histological Observations

For the histological observation of the endothelium, corneas were fixed in Carnoy's solution overnight and rehydrated through a descending alcohol series. Corneas were dissected free of their surrounding scleral rim, and the endothelial cell layer, along with Descemet's membrane, were gently separated from the rest of the tissue. Isolated tissues were flat mounted on albumin-coated glass slides and received 4–5 radial cuts to allow them to lie flat. Tissues were then stained with 1% cresyl violet acetate (Eastman Kodak Co., Rochester, NY), and mounted in Permount (Fisher Scientific, Fair Lawn, NJ).

Cytoskeletal Visualization

Microfilaments were visualized with either TRITC or FITC phalloidin (Molecular Probes, Junction City, OR) as described [Gordon and Staley, 1990]. Briefly, cultured tissues were gently rinsed in 0.1M PBS and fixed in 3.7% formaldehyde (Fisher Scientific) for 10 min at room temperature. Following a 30-min PBS wash, flat mounts were prepared and allowed to air dry. Tissues were then extracted in acetone (−10°C) and subsequently rinsed in 0.1M PBS for 10 min. Endothelia were exposed to 1.67×10^{-7}M phalloidin in 0.1M PBS for 30 min, rinsed and mounted in a p-phenylenediamine/glycerol anti-fading solution [Johnson and Araujo, 1982].

For microtubule localization, fixation and extraction of the tissue were identical to that described for microfilaments. Microtubules were stained with Tu-27B, a monoclonal antibody to β-tubulin (a generous gift of Dr. L.I. Binder, Northwestern University), followed by staining with a 1:16 dilution of rabbit anti-mouse IgG-rhodamine (ICN) using standard immunocytochemical protocols. Endothelial flat mounts were sealed using the anti-fading medium described above.

Biochemical Analysis

For analysis of the endothelial cytosolic protein profile, tissues were isolated from corneas and homogenized on ice for 15 min in 0.1M Tris buffer containing 0.1% SDS and the following protease inhibitors: aprotinin (1 mg/ml), leupeptin (1 µg/ml), pepstatin (0.7 µg/ml), and phenylmethylsulfonylfluoride (PMSF; 2 mM). Following protein determination using the DC protein assay (Bio-Rad Laboratories, Hercules, CA), β-mercaptoethanol was added to the sample to give a final concentration of 2%. Samples were boiled for 5 min, cooled, and centrifuged to remove any particulate material. Between 70–100 µg of cytosolic protein was loaded onto and separated on 10% polyacrylamide mini gels (0.375M Tris HCl, pH 8.8) with an overlying 4% stacking gel and subsequently stained with Brilliant Blue G concentrate (Sigma). To identify the actin and tubulin band within the cytosolic profile, proteins were electrophoretically transferred onto Immobilon P® membranes (Millipore Corporation, Bedford, MA) and exposed to either anti-actin (ICN) or Tu-27B, respectively. This was followed by incubation in goat anti-rabbit IgG-HRP or Protein G-HRP (both from Bio-Rad) and visualized with diaminobenzidine as the substrate.

Immunoprecipitation

Endothelia were isolated and homogenized for 30 min on ice in 10 mM Tris HCl containing 0.05% Nonidet P-40 (pH 7.2) with 0.15M NaCl, 1 mM $CaCl_2$, 1 mM EDTA, 4 mM PMSF, and 0.02% sodium azide. Following centrifugation to remove Descemet's membrane, actin or tubulin was immunoprecipitated using either anti-actin (IgG fraction; Biomedical Technologies, Stoughton, MA) or Tu-27B, respectively. Samples were incubated overnight at 4°C with agitation to optimize antibody/antigen interaction. Immune complexes were then incubated in Protein A-sepharose CL-4B beads (Pharma-

cia LKB, Uppsala, Sweden) and isolated by centrifugation. The ensuing pellet was washed and dissolved in Tris sample buffer containing 1% SDS without β-mercaptoethanol. Following the determination of protein concentration, approximately 7 μg of protein was loaded onto gels as described above and subsequently electrophoresed by SDS-PAGE.

Scintillation Analysis

Actin and tubulin immunoprecipitates were analyzed by liquid scintillation counting using a 1214 Rackbeta liquid scintillation counter (LKB/Wallac). Seven micrograms of each protein sample were dissolved in 10 ml of ACS scintillation fluid (Dupont/NEN, Boston, MA). Counts were adjusted for background and given as counts/μg protein.

Autoradiography

Gels containing ^{35}S-labeled proteins were placed in cellophane (BioDesign, Inc., Carmel, NY), dried overnight and placed in film cassette holders with RX medical X-Ray film (Fuji,). Film was exposed up to 1 week at −40°C and developed with Kodak D-19 developer.

RESULTS

Endothelial Wound Repair

The entire adult noninjured corneal endothelium is composed of a monolayer of non-cycling, tightly packed polyhedral cells containing oval to kidney shaped nuclei (Fig. 1A). A freeze injury to the tissue (Fig. 1B,C) produces a distinct wound border between the cells and the denuded injury zone, where the underlying Descemet's membrane is exposed. At 24 h after injury (Fig. 1D), cells adjacent to the wound have begun to separate from the rest of the monolayer and initiate movement into the injury zone. By 48 h after wounding, extensive inward movement has occurred within the injury area (Fig. 1E) and Descemet's membrane has nearly been re-epithelialized by the cells.

Biochemical examination of the Coomassie blue stained cytosolic protein profile (Fig. 2, lanes 2–4) indicated variations in the pattern of endothelial proteins between noninjured tissues and tissues undergoing wound repair. Autoradiographic analysis of metabolic labeled tissues (Fig. 2, lanes 5–7) shows that more extensive changes were apparent relative to the synthesis of various proteins within the bands.

Cytoskeletal Changes Accompanying Wound Repair

The injury-induced migratory response of corneal endothelial cells is accompanied by cytoskeletal reorganization. Morphologically, microfilament pattern changes are much more extensive than are those of microtubules. In the noninjured endothelium (Fig. 3A) phalloidin staining reveals a pattern of circumferential microfilament bundles within the cells that is observed throughout the tissue. Twenty-four hours after a circular freeze wound, cells adjacent to the wound border begin to migrate into the injury. By this time microfilaments have reorganized into stress fibers (Fig. 3B) that are orientated in the direction of the cells broad-based lamellipodia. By 48 h post-injury (Fig. 3C), these cells have migrated far into the wound region, nearly covering the defect, and still display prominent stress fibers.

Microtubule rearrangements in migrating endothelial cells appear much more subtle. Immunofluorescent microscopy of the noninjured tissue demonstrates that cells are tightly packed and exhibit an extensive microtubular network (Fig. 3D). By 24 h after an injury, cells surrounding the wound display distinct MTOCs that are oriented towards the wound region (Fig. 3E). When observed at 48 h after injury, the microtubule patterns are somewhat masked due to the extensive disorganization within the wound region (Fig. 3F), but spindles, where present, are readily visible (Fig. 3F, inset).

Phalloidin Effect on Cytoskeletal Reorganization During Wound Repair

Incubation of organ cultured endothelium in 7.5 μM TRITC-phalloidin for 20 h ("pre-treated"), results in toxin uptake and the staining of the cells circumferential microfilament networks (Fig. 4A) in a pattern reminiscent to that seen after the staining of fixed preparations. Pre-treated tissues that were subsequently injured and cultured for up to 48 h and examined after fixation showed dramatic changes relative to microfilament reorganization. When observed at 24 and 48 h after injury, endothelial cells exhibited few, if any, stress fibers within their cytoplasm (Figs. 4B,C). In order to investigate whether the lack of visible stress fibers could be explained simply as a loss of label, experiments were repeated using non-labeled phalloidin followed by post-fixation staining with fluorochrome conjugated phalloidin. When these tissues were examined, only

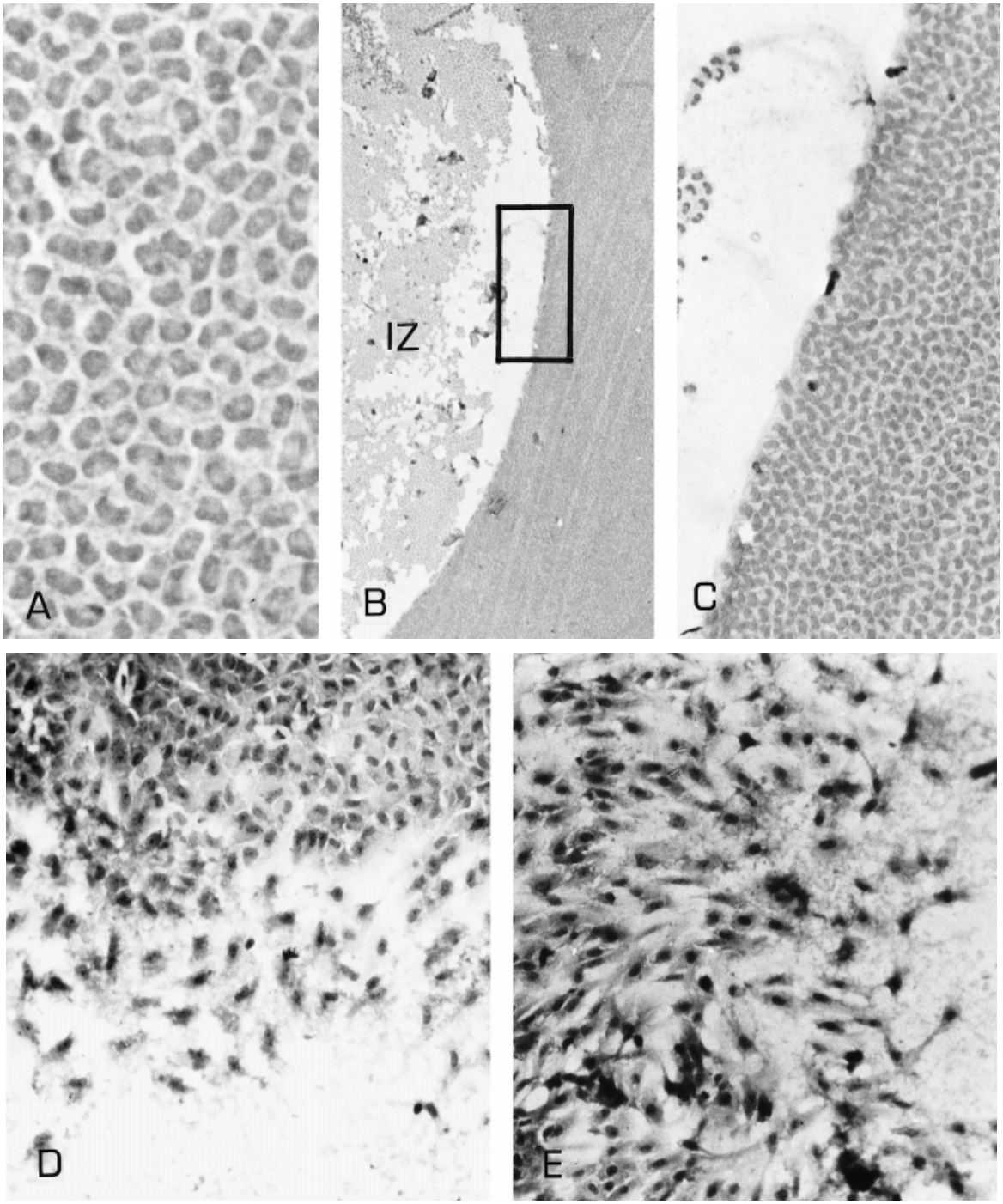

Fig. 1. Wound response in the organ-cultured rabbit corneal endothelium. **A:** Flat mount of the noninjured endothelium. Note the monolayer, composed of closely packed polyhedral cells, does not contain any cells undergoing mitosis. **B:** The injury zone (IZ) is clearly delineated following a circular freeze wound. **C:** Higher magnification of rectangular region seen in B. **D:** Twenty-four hours after injury, cells surrounding the wound have begun to migrate inward toward the center of the wound. **E:** By 48 h post-injury, the wound is nearly filled in and extensive migration is observed. Original magnifications: A, ×130; B, ×10; C, ×32; D, E, ×80.

diffuse fluorescence could be observed at 24 h post-injury (Fig. 4D), but, after 48 h, staining revealed the presence of distinct stress fibers within the cells (Fig. 4E). Similar results were obtained with preparations that were pre-treated with TRITC-phalloidin before injury and post-stained with FITC-phalloidin after the conclusion of the experiment. Here, cells showed a distinct lack of TRITC-phalloidin stained stress fibers at 48 h post-injury (Fig. 4F),

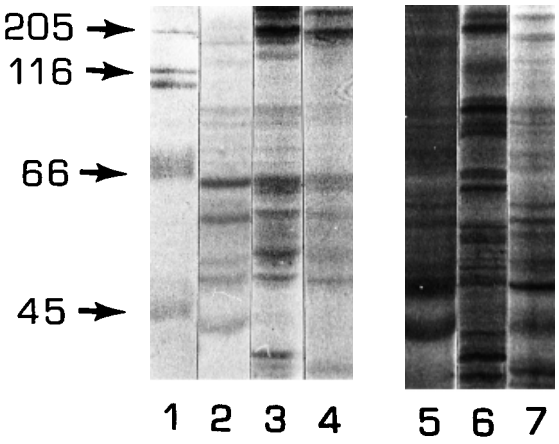

Fig. 2. Detection of rabbit corneal endothelial tissue proteins by 10% SDS-PAGE and ^{35}S metabolic labeling. **Lanes 1–4** are stained with Coomassie blue. Lane 1, protein standards; lanes 2–4, 0, 24, and 48 h post-injuries, respectively. **Lanes 5–7,** the corresponding autoradiographic patterns from 0, 24, and 48 h post-injuries.

whereas, FITC-phalloidin staining revealed numerous stress fibers within the cytoplasm (Fig. 4F).

Actin and Tubulin Synthesis During Endothelial Cell Migration

Rabbit corneal endothelial cell actin and tubulin were characterized using SDS-PAGE, anti-actin and anti-tubulin immunoblotting and immunoprecipitation. When immunoblotted cytosolic proteins were compared to molecular weight standards, two bands were detected at approximately 45 kD and near 50 kD, corresponding to the molecular weights of actin and tubulin, respectfully (Fig. 5). Electrophoresis of immunoprecipitated actin and tubulin from endothelial cells resulted in bands whose migration paralleled results obtained by Western blots (Fig. 5). Densitometric scans (data not shown) of the Coomassie blue stained cytoplasmic profile determined that actin comprised approximately 10% of the total soluble protein, whereas, tubulin constituted about 4.8%.

Metabolically labeled actin and tubulin were immunoprecipitated from pooled tissues of either noninjured, 24- or 48-h post-injured endothelial preparations. Immunoprecipitates of actin and tubulin from noninjured tissues exhibited very little incorporation of ^{35}S (Tables I and II) and neither protein was detected on autoradiograms of the gels (Fig. 6). When analysis was performed on pooled preparations from 24 or 48 h post-injured tissues, once again, neither actin nor tubulin immunoprecipitates were detected by autoradiographic imaging (Fig. 6). Low isotope incorporation was verified by liquid scintillation counting (Tables I and II) that indicated ^{35}S uptake into actin and tubulin did not significantly differ during wound repair from those levels observed in noninjured tissues.

When actin and tubulin reorganization was impaired using either phalloidin pre-treatment or colchicine, respectively, high levels of ^{35}S incorporation were detected at 48 h post-injury for each protein (Tables I and II) and their respective immunoprecipitates were clearly visible on autoradiograms (Fig. 6). Furthermore, incubating injured tissues in media containing 0.01 μg/ml AMD for the final 30 h of culture (for a total culture time of 48 h), greatly surpressed ^{35}S incorporation into both actin and tubulin (Tables I and II). Fluorescent observations of actin in cells treated by this protocol show that cells contained some microfilaments (Fig. 7A), but far less than their control counterparts (Fig. 7B).

DISCUSSION

Results presented here indicate that corneal endothelial cytoskeletal reorganization during cell migration, in response to a circular freeze injury, is not dependent on de novo synthesis of actin or β-tubulin, since labeled material was not detected following immunoprecipitation of either protein. However, the synthesis of each protein was heightened by interfering with the reorganization of its respective filament system. Pre-incubating tissues in phalloidin prior to injury prevented subsequent microfilament reorganization and resulted in the synthesis of actin. Likewise, incubation of endothelia in medium containing colchicine also resulted in a significant incorporation of label into immunoprecipitated tubulin. In both cases, treatment with actinomycin D suppressed isotope incorporation, suggesting that the synthesis of each protein resulted, at least in part, from new gene expression rather than post-transcriptional changes of pre-existing m-RNA.

Injured corneal endothelial cells adjacent to the wound edge undergo striking modifications in their actin organization. Initially, these cells exhibit apical CMBs, but as migrating cells, actin is reorganized into distinct stress fibers [Gordon and Staley, 1990; Ichijima et al., 1993], implying that actin reorganization may involve the depolymerization of the apical microfilament bundle. Our results suggest that CMB depolymerization is central to actin reorganization and is probably sufficient enough to in-

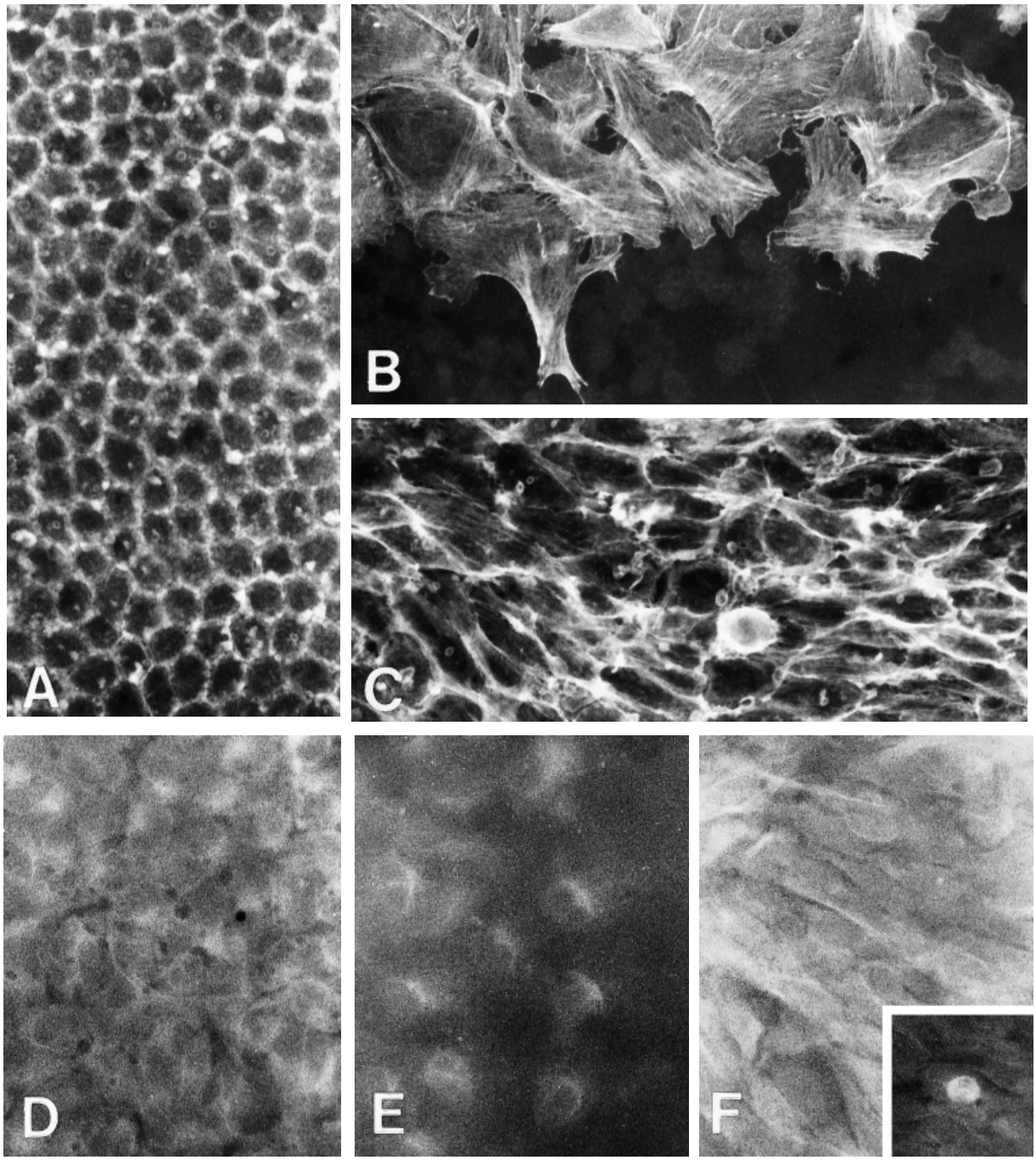

Fig. 3. Microfilament and microtubule changes accompanying rabbit corneal wound repair. In noninjured tissue (**A**), the circumferential microfilament bundles of the cells can be observed following rhodamine phalloidin staining. **B:** Twenty-four hours after a circular freeze wound, cells migrating into the injury area exhibit stress fibers but not circumferential microfilament bundles. **C:** Forty-eight hours after injury, cells have migrated into the wound region as the monolayer becomes reestablished. **D:** Immunofluorescence of microtubule distribution in noninjured tissue. The closely packed cells display a crowded distribution of microtubules. **E:** Twenty-four hours after injury, cells preparing to migrate into the wound orientate MTOCs in the direction of their movement. **F:** By 48 h post-injury, microtubule patterns are difficult to see because of the disorganization within the injury zone. Inset: mitotic spindle of a dividing cell. Original magnifications: A, C–F, ×128; B, ×200.

crease the monomeric G-actin pool size, thus curtailing additional actin synthesis, and promote stress fiber assembly. Indeed, reversible dynamics between G-actin, F-actin, and their associated proteins serve as the basis for actin function [Korn, 1982; Cooper, 1991]. Endothelia pre-treated with TRITC-phalloidin displayed no labelled stress fibers at either 24 or 48 h post-injury, suggesting that the toxin stabilized the CMB, thereby preventing its depolymeriza-

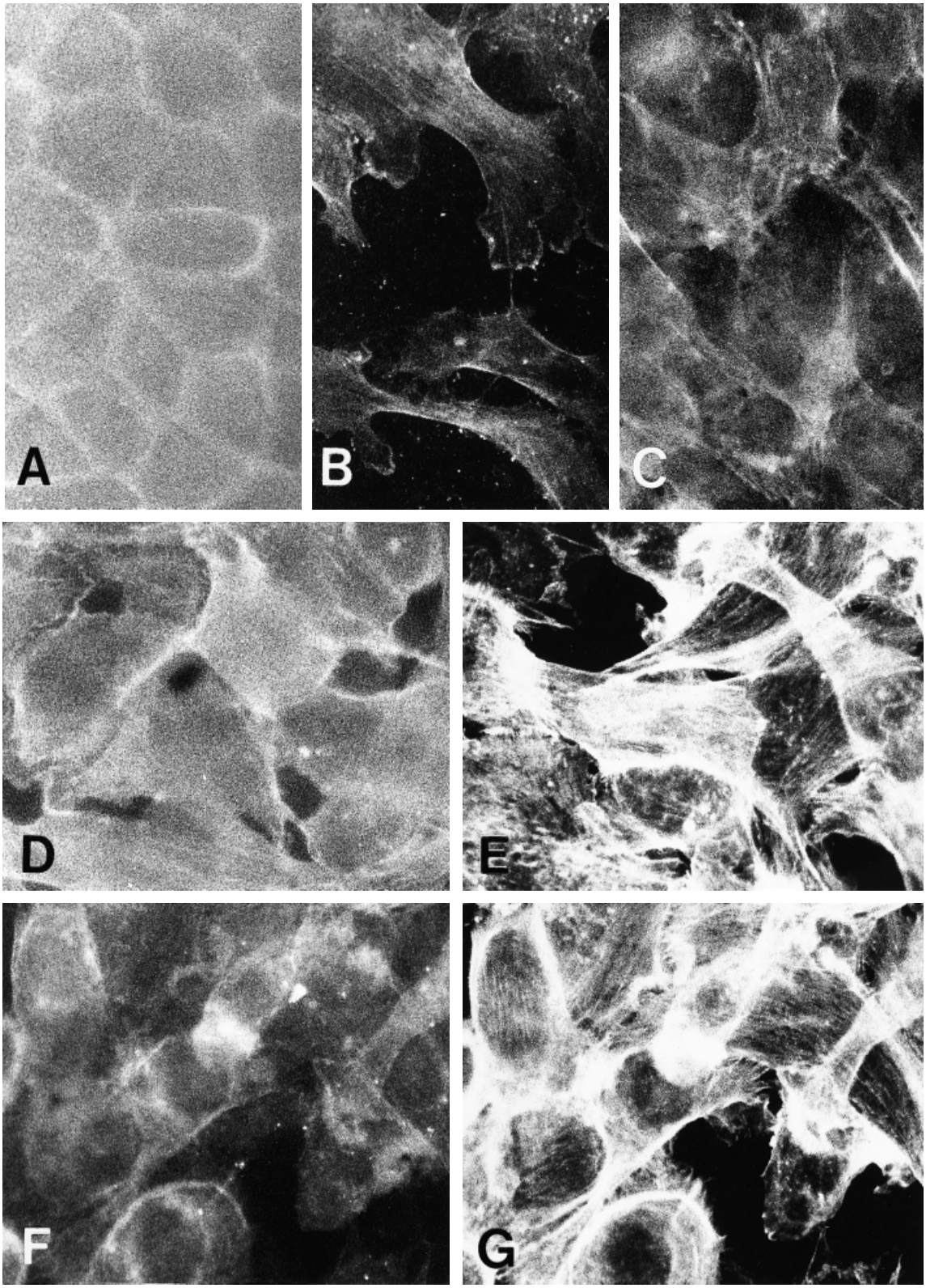

Fig. 4. Effect of phalloidin pre-treatment on corneal endothelial actin reorganization following a circular freeze wound. **A:** Incubating tissues with rhodamine labeled phalloidin for 20 h stains the circumferential microfilament bundles similar to that seen using post-fixation staining. **B,C:** Fluorescent micrographs of endothelial cells pre-incubated for 20 h in rhodamine phalloidin, injured, and fixed at 24 and 48 h after injury, respectively. In both cases, cells exhibit very few rhodamine phalloidin positive stress fibers in their cytoplasm. **D,E:** Fluorescent micrographs of tissues pre-treated in non-labeled phalloidin for 20 h, injured, and cultured for either 24 or 48 h, then fixed and post-stained with labeled phalloidin. At 24 h after wounding (D) only diffuse fluorescence is observed and stress fibers are not evident; however, cells in 48-h post-injured preparations (E), display prominent stress fibers. **F,G:** Preparations that were initially pre-treated in rhodamine phalloidin for 20 h, injured, and fixed after 48 h show no evidence of stress fibers (F). However, when the same tissue is subsequently stained with fluorescein phalloidin (G), distinct stress fibers are now detected. Original magnifications: A–G, ×200.

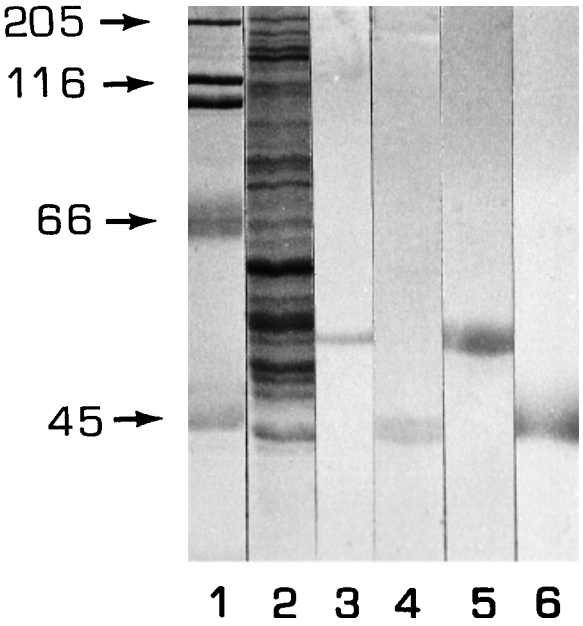

Fig. 5. Characterization of rabbit corneal endothelial tubulin and actin by SDS-PAGE and immunoblotting. **Lane 1,** Coomassie brilliant blue G stained protein standards; **lane 2,** endothelial cell protein profile; **lane 3,** immunoblotting of tubulin; **lane 4,** immunoblotting of actin; **lane 5,** immunoprecipitation of endothelial tubulin; **lane 6,** immunoprecipitation of endothelial actin.

tion and subsequent actin reorganization. Similar work by Serpinskaya et al. [1990], demonstrated that phalloidin loading into cultured embryonic mouse fibroblasts increased polymerized actin within cells while decreaseing monomeric levels. This change was accompanied by a 2–3-fold increase in actin synthesis. Reuner et al. [1995a,b] demonstrated that phalloidin treatment promotes F-actin assembly by driving the polymerization of the pre-existing G-actin, and provided evidence that the G-actin level may serve to regulate actin synthesis in a negative feedback manner [Reuner et al., 1991, 1996]. Hepatocytes treated with phalloidin decreased their G-actin/F-actin ratio but increased their actin mRNA levels, whereas treatment with Clostridium botulinum C2 toxin increased the G-actin/F-actin ratio but decreased actin mRNA [Reuner et al., 1991]. Furthermore, any increases in actin mRNA levels were blocked by actinomycin D exposure [Reuner et al., 1995a], suggesting that increased actin synthesis was the result of new transcription. The results of these studies taken together indicate that any agent capable of shifting the G-actin/F-actin ratio should significantly affect the levels of actin synthesis. Recently, Cappelletti et al. [1996] showed this to be the case with A549 human lung carcinoma cells treated with the oxidant agent paraquat. Paraquat was shown to promote the assembly of numerous single microfilaments throughout the cytoplasm with a parallel decrease in the monomeric actin level, creating a shift in the G-actin/F-actin ratio. This ratio change was then followed by strong de novo actin synthesis [Cappelletti et al., 1996].

TABLE I. Actin Synthesis*

Hours after injury	Treatment	CPM/μg protein	n-value
0	None	36.16 ± 11.47	4
24	None	33.37 ± 11.99	3
48	None	31.25 ± 4.59	2
48	7.5 μM phalloidin	16,418.65 ± 9,884.62	2
48	7.5 μM phalloidin + AMD	232.69 ± 44.46	2

*Corneas were cultured in 10% rabbit serum for all experiments and treated as indicated. Tissues were labeled with ^{35}S for the final 6 h of culture and subsequently immunoprecipitated. Where noted, 0.01 μg/ml actinomycin (AMD) was added to cultures at 18 h post-injury for the duration of the experiment. During wound repair (0, 24, 48 h post-injury) only minimal ^{35}S incorporation into actin was observed. When corneas were pre-loaded with 7.5 μM phalloidin for 20 h, injured and cultured under normal conditions, a significant increase in incorporation occurs. Corneas preloaded with 7.5 μM phalloidin for 20 h, injured and cultured in the presence of AMD, show a significant decrease in ^{35}S incorporation. Each n-value represents 10 pooled endothelium.

TABLE II. Tubulin Synthesis*

Hours after injury	Treatment	CPM/μg protein	n-value
0	None	26.76 ± 21.23	4
24	None	25.99 ± 24.47	3
48	None	32.71 ± 15.96	2
48	10^{-8}M colchicine	3,195.94 ± 1,928.93	2
48	10^{-8}M colchicine + AMD	85.97 ± 1.39	2

*Corneas were cultured in 10% rabbit serum for all experiments and treated as indicated. Tissues were labeled with ^{35}S for the final 6 h of culture and subsequently immunoprecipitated. Where noted, 0.01 μg/ml actinomycin (AMD) was added to cultures at 18 h post-injury for the duration of the experiment. During wound repair (0, 24, 48 h post-injury) only minimal ^{35}S incorporation into tubulin was observed. When corneas were injured and cultured in the presence of 10^{-8}M colchicine, a significant increase in incorporation occurs. Corneas injured and cultured in the presence of 10^{-8}M colchicine and AMD show a significant decrease in ^{35}S incorporation. Each n-value represents 10 pooled endothelium.

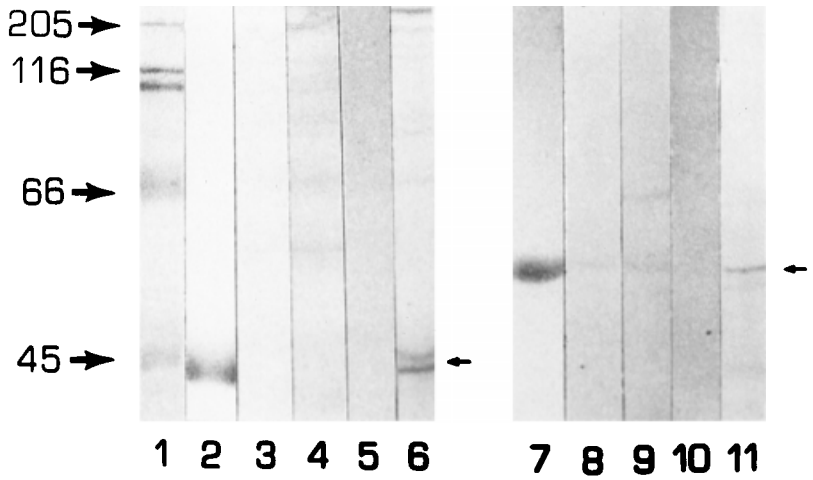

Fig. 6. Autoradiographs of ^{35}S-Trans® incorporation into immunoprecipitated actin and tubulin during organ cultured corneal endothelial wound repair. **Lane 1,** Coomassie brilliant blue G stained standards; **lane 2,** immunoprecipitation of actin, **lanes 3–5** autoradiographs of actin immunoprecipitates at 0, 24, and 48 h after injury; **lane 6,** autoradiograph of actin immunoprecipitate 48 h post-injury following pre-treatment with 7.5 μM phalloidin prior to wounding; **lane 7,** tubulin immunoprecipitation; **lanes 8–10,** autoradiographs of tubulin immunoprecipitates at 0, 24, and 48 h after injury; **lane 11,** autoradiograph of tubulin immunoprecipitated 48 h post-injury. Tissues were organ cultured in the presence of 10^{-8}M colchicine.

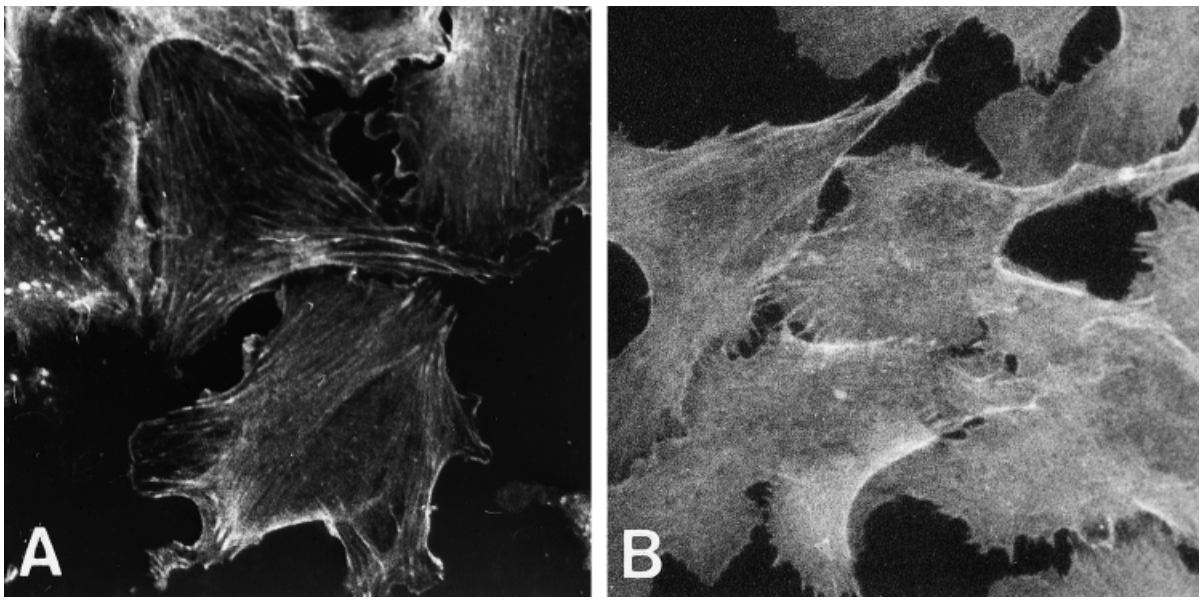

Fig. 7. Actinomycin D exposure for the final 30 h of organ culture, in tissues pre-treated with phalloidin prior to injury. Note the greatly reduced numbers of stress fibers in the actinomycin D exposed tissue (**A**) when compared to the control tissue (**B**) that did not receive the drug.

Our actin results parallel the above findings. Although we did not measure G-actin pools in our system, phalloidin treatment probably causes a similar decline in the G-actin/F-actin ratio by inducing actin polymerization, leading to a dramatic upregulation in actin synthesis and probably actin mRNA transcription. On the other hand, the increased availability of G-actin provided by the disassembly of the CMB probably suppresses actin mRNA levels and explains why very low levels of radiolabelled actin immunoprecipitate were detected during the course of wound repair in non-phalloidin-treated tissues. In contrast, disrupting CMB depolymerization with phalloidin probably leads to decreased G-actin levels and concomitant increases in actin mRNA levels. This would account for the large incorporation of radiolabel

into actin immunoprecipitates as well as the appearance of new stress fibers (as detected by post-fixation staining) in phalloidin-treated cells at 48 h post-injury. Furthermore, because actimomycin D treatment suppresses ^{35}S incorporation into actin immunoprecipitates, it appears likely that increased synthesis is due primarily to new transcription and not necessarily the result of any longed-lived mRNA.

Results obtained with β-tubulin paralleled those of actin in that the initiation of new synthesis appears dependent on interfering with microtubule reorganization during wound repair. In the normal repair process, immunoprecipitation of labelled β-tubulin gave virtually little or no S^{35} incorporation. In contrast, exposure of endothelia during wound repair to 10^{-8}M colchicine, which is sufficient to cause the total loss of immunofluorescent microtubular staining [Gordon and Staley, 1990], prompted a large increase in isotope incorporation into immunoprecipitates by 48 h post-injury. It therefore appears that colchicine induced depolymerization of microtubules, in a temporal dependent manner, can subsequently upregulate β-tubulin synthesis.

Microtubules are characterized by "dynamic instability," the assembly and disassembly of microtubules that involve rapid exchanges of subunits between the polymerized and nonpolymerized (soluble) tubulin pool [Cassimeris, 1993; Gelfand and Bershadsky, 1991; Cassimeris et al., 1987; Mitchison and Kirschner, 1984]. Recent work [Panda et al., 1994] suggests that the dynamic properties and functions of microtubules may be, in part, dictated by the relative amounts of different tubulin isotypes. The synthesis of β-tubulin is under autoregulatory control, whereby its synthesis is dependent on the ratio between free tubulin subunits and the polymerized state [Caron et al., 1985b; Cleveland et al., 1983; Ben'Zev et al., 1979], with the free tubulin, in turn, capable of regulating the stability and levels of its own mRNA [Bachurski et al., 1994; Cleveland et al., 1981; Pachter et al., 1987]. In contrast, α-tubulin appears to limit its own synthesis by repressing its translation [Gonzalez-Garay and Cabral, 1996] in a process that may act as part of a mechanism to maintain the coordinated syntheses of α- and β-tubulins, thus ensuring that appreciable levels of free α- or β-tubulins do not occur [Gonzalez-Garay and Cabral, 1995, 1996].

Previous short-term (≤6 h) studies with colchicine [Ben Ze'ev et al., 1979; Caron et al., 1985b] demonstrated that depolymerizing microtubules increased the level of soluble tubulin and depressed its synthesis. This was subsequently confirmed by microinjecting purified tubulin subunits into cultured cells [Cleveland et al., 1983]. Longer treatment with low doses of colcemid resulted in reduced microtubular lengths, thus lowering polymer mass and decreasing tubulin synthesis by a small percentage that remained proportionate to soluble tubulin levels [Caron et al., 1985a]. In contrast, vinblastine exposure disrupts microtubules but forms aberrant aggregations of tubulin as "paracrystalline" structures that decrease the subunit pool and stimulate synthesis [Ben'Zev et al., 1979].

Our data initially appear to contradict the above findings but, in fact, do support them. There is no doubt that short-term incubation with colchicine initially increases the free tubulin pool and reduces tubulin synthesis. Findings presented here demonstrate the reverse effect, that is, alteration of free tubulin subunits with colchicine, so that they become ineffective in microtubular dynamics, initiates the upregulation of tubulin synthesis. Since microtubules play pivitol roles for cell movement in the corneal endothelium during wound repair [Sabet and Gordon, 1989], and in other systems as well [Liao et al., 1995], there is a critical need to maintain a viable subunits pool. Colchicine-tubulin complexes are known to bind microtubules at either end in vitro, reducing their growth rate [Vandecandelaere et al., 1994]. Long-term colchicine incubation produces a transmuted pool of tubulin subunits that effects the free/polymerized subunit ratio, and subsequently results in the upregulation of tubulin transcription, analogous to vinblastine treatment [Ben'Zev et al., 1979]. Thus, in response to colchicine, cells initially react to increased free tubulin levels and decrease tubulin synthesis. However, since colchicine-tubulin complexes neither polymerize nor support microtubular dynamic instability [Vandecandelaere et al., 1994], and effectively decrease the viable free tubulin pool, the cell has no choice but to upregulate tubulin synthesis.

ACKNOWLEDGMENTS

The authors thank Dr. Lester I. Binder, Department of Cell and Molecular Biology, North-

western University, for his generous gift of Tu-27B antibody.

REFERENCES

Bachurski CJ, Theodorakis NG, Coulson RMR, Cleveland DW (1994): An amino-terminal tetrapeptide specifies cotranslational degradation of β-tubulin but not α-tubulin mRNAs. Mol Cell Biol 14:4076–4086.

Barry PA, Petroll WM, Andrews PM, Cavanagh HD, Jester JV (1995): The spatial organization of corneal endothelial cytoskeletal proteins and their relationship to the apical junctional complex. Invest Ophthalmol Vis Sci 36:1115–1124.

Bement WM, Forscher P, Mooseker, MS (1993): A novel cytoskeletal structure involved in purse string wound closure and cell polarity maintenance. J Cell Biol 121:565–578.

Ben'Zev A, Farmer SR, Penman S (1979): Mechanisms of regulating tubulin synthesis in cultured mammalian cells. Cell 17:319–325.

Cappelletti G, Maggioni MG, Carnevali DC, Bonasoro F, Maci R (1996): Dynamic changes in the state of actin polymerization in human alveolar cells exposed to the oxidant agent paraquat. Eurp J Cell Biol 71:293–302.

Caron JM, Jones AL, Kirschner MW (1985a): Autoregulation of tubulin synthesis in hepatocytes and fibroblasts. J Cell Biol 101:1763–1772.

Caron JM, Jones AL, Rall LB, Kirschner MW (1985b): Autoregulation of tubulin synthesis in enucleated cells. Nature 317:648–651.

Cassimeris L (1993): Regulation of microtubule dynamic instability. Cell Motil Cytoskeleton 26:275–281.

Cassimeris LU, Walker RA, Pryer NK, Salmon ED (1987): Dynamic instability of microtubules. BioEssays 7:149–154.

Cleveland DW, Lopata MA, Sherline P, Kirschner MW (1981): Unpolymerized tubulin modulates the level of tubulin mRNAs. Cell 25:537–546.

Cleveland DW, Pittenger MF, Feramisco JR (1983): Elevation of tubulin levels by microinjection suppresses new tubulin synthesis. Nature 305:738–740.

Cooper JA (1991): The role of actin polymerization in cell motility. Ann Rev Physiol 53:585–605.

Doughman DJ, Van Horn DL, Rodman WP, Byrnes P, Linstrom RL (1976): Human corneal endothelial layer repair during organ culture. Arch Ophthalmol. 94:1791–1796.

Ettenson DS, Gotlieb AI (1993a): In vitro large-wound re-endothelialization. Inhibition of centrosome redistribution by transient inhibition of transcription after wounding prevents rapid repair. Arterioscler Thromb 13:1270–1289.

Ettenson DS, Gotlieb AI (1993b): Role of endothelial cells in vascular integrity and repair in artherosclerosis. Adv Pathol Lab Med 6:285–309.

Gabbiani G, Gabbiani F, Lombardi D, Schwartz SM (1983): Organization of actin cytoskeleton in normal and regenerating arterial endothelial cells. Proc Natl Acad Sci USA 80:2361–2364.

Gelfand VI, Bershadsky AD (1991): Microtubule dynamics: Mechanism, regulation, and function. Annu Rev Cell Biol 7:93–116.

Gonzalez-Caray ML, Cabral F (1995): Overexpression of an epitope-tagged β-tubulin in Chinese hamster ovary cells causes an increase in endogeneous α-tubulin synthesis. Cell Motil Cytoskeleton 31:259–272.

Gonzalez-Garay ML, Cabral F (1996): α-Tubulin limits its own synthesis: Evidence for a mechanism involving translation repression. J Cell Biol 135:1525–1534.

Gordon SR (1988): Changes in the distribution of extracellular matrix proteins during wound repair in corneal endothelium. J Histochem Cytochem 36:409–416.

Gordon SR (1990): Changes in extracellular matrix proteins and actin during corneal endothelial growth. Invest Ophthalmol Vis Sci 31:94–101.

Gordon SR (1994): Cytological and immunocytological approaches to the study of corneal endothelial wound repair. Prog Histochem Cytochem 28:1–66.

Gordon SR, Rothstein H (1978): Studies on corneal endothelial growth and repair. I. Microfluorometric and autoradiographic analyses of DNA synthesis, mitosis and amitosis following freeze injury. Metabol Ophthalmol 2:57–63.

Gordon SR, Rothstein H (1982): Studies on corneal endothelial growth and repair. III. Effects of DNA and RNA synthesis inhibitors upon restoration of transparency following injury. Ophthalmol Res 14:195–209.

Gordon SR, Staley CA (1990): Role of cytoskeleton during injury-induced cell migration in corneal endothelium. Cell Motil Cytoskeleton 16:47–57.

Gordon SR, Essner E, Rothstein H (1982): In situ demonstration of actin in normal and injured ocular tissues using 7-nitrobenz-2-oxa-1,3-diazole phallacidin. Cell Motil 2:343–354.

Gotlieb AI, Spector W, Wong MKK, Lacey C (1984): In vitro reendothelialization. Microfilament bundle reorganization in migrating porcine endothelial cells. Arteriosclerosis 4:91–96.

Hergot GJ, Sandig M, Kalnins VI (1989): Cytoskeletal organization of migrating retinal pigment epithelial cells during wound healing in organ culture. Cell Motil Cytoskeleton 13:83–93.

Ichijima H, Petroll WM, Barry PA, Andrews PM, Dai M, Cavanagh HD, Jester JV (1993): Actin filament organization during endothelial wound healing in the rabbit cornea: Comparison between transcorneal freeze and mechanical scrape injuries. Invest Opthalmol Vis Sci 34: 2803–2812.

Johnson GD, Araujo GMDN (1982): A simple method of reducing the fading of immunofluorescence during microscopy. J Immunol Methods 43:349–350.

Korn ED (1982): Actin polymerization and its regulation by proteins from nonmuscle cells. Physiol Rev 62:672–737.

Lee T-YJ, Rosenthal A, Gotlieb AI (1996): Transition of aortic endothelial cells from resting to migrating cells is associated with three sequential patterns of microfilament organization. J Vasc Res 33:13–24.

Liao G, Nagasaki T, Gundersen GG (1995): Low concentrations of nocodazole interfere with fibroblast locomotion without significantly affecting microtubule level: Implications for the role of dynamic microtubules in cell locomotion. J Cell Sci 108:3473–3483.

Martin P, Lewis J (1992): Actin cables and epidermal movement in embryonic wound healing. Nature 360:179–182.

Mitchison TJ, Kirschner MW (1984): Dynamic instability of microtubule growing. Nature 312:237–242.

Munjal ID, Blake DA, Sabet MD, Gordon SR (1990): Thrombospondin: Biosynthesis, distribution, and changes associated with wound repair in corneal endothelium. Eur J Cell Biol 52:252–263.

Nusrat A, Delp C, Madara JL (1992): Intestinal epithelial restitution. Characterization of a cell culture model and mapping of cytoskeletal elements in migrating cells. J Clin Invest 89:1501–1511.

Pachter JS, Yen TJ, Cleveland DW (1987): Autoregulation of tubulin expression is achieved through specific degradation of polysomal tubulin mRNAs. Cell 51:283–292.

Panda D, Miller HP, Banerjee A, Luduéna, Wilson L (1994): Microtubule synamics in vitro are regulated by the tubulin isotype composition. Proc Natl Acad Sci USA 91:11358–11362.

Petroll WM, Jester JV, Barry-Lane P, Cavanagh HD (1995): Assessment of F-actin organization and apical-basal polarity during in vivo cat endothelial wound healing. Invest Ophthalmol Vis Sci 36:2492–2502.

Petroll WM, Barry-Lane PA, Cavanagh HD, Jester JV (1997): ZO-1 Reorganization and myofibroblast transformation of corneal endothelial cells after freeze injury in the cat. Exp Eye Res 64:257–267.

Reuner, KH, Schlegel K, Just I, Aktories K, Katz N (1991): Autoregulatory control of actin synthesis in cultured rat hepatocytes. FEBS Lett 286:100–104.

Reuner KH, Wiederhold M, Dunker P, Just I, Bohle RM, Kröger M, Katz N (1995a): Autoregulation of actin synthesis in hepatocytes by transcriptional and posttranscriptional mechanisms. Eur J Biochem 230:32–37.

Reuner KH, Wiederhold M, Schlegel K, Just I, Katz N (1995b): Autoregulation of actin synthesis by physiological alterations of the G-actin level in hepatocytes. Eur J Clin Chem Clin Biochem 33:569–574.

Reuner KH, Dunker P, van der Does A, Wiederhold M, Just I, Aktories K, Katz N (1996): Regulation of actin synthesis in rat hepatocytes by cytoskeletal rearrangements. Eur J Cell Biol 69:189–196.

Rogers KA, Sandig M, McKee NH, Kalnins VI (1989): The distribution of microfilament bundles in rabbit endothelial cells in the intact aorta and during wound healing in situ. Biochem Cell Biol 67:553–562.

Sabet MD, Gordon SR (1989): Ultrastructural immunocytochemical localization of fibronectin deposition during corneal endothelial wound repair. Evidence for cytoskeletal involvement. Biol Cell 65:171–179.

Serpinskaya AS, Denisenko ON, Gelfand VI, Bershadsky AD (1990): Stimulation of actin synthesis in phalloidin-treated cells. Evidence for autoregulatory control. FEBS Lett 277:11–14.

Vandecandelaere A, Martin SR, Schilstra MJ, Bayley PM (1994): Effects of the tubulin-colchicine complex microtubule dynamic instability. Biochem 33:2972–2801.

Wong MKK, Gotlieb AI (1988): The reorganization of microfilaments, centrosomes, and microtubules during in vitro small wound reendothelialization. J Cell Biol 107:1777–1783.

Zahm J-M, Chevillard M, Puchelle E (1991): Wound repair of human surface respiratory epithelium. Am J Respir Cell Biol 5:242–248.